Cooperative Effects in the $[Fe(mtz)_6](BF_4)_2$ Spin-Crossover System: Fine Tuning the Energy Gap

Roland Hinek and Philipp Gütlich

Institut für Anorganische Chemie und Analytische Chemie, Johannes-Gutenberg-Universität,
Staudingerweg 9, 6500 Mainz, Germany

Andreas Hauser*

Institut für anorganische und physikalische Chemie, Universität Bern,
Freiestrasse 3, 3000 Bern 9, Switzerland

Received May 4, 1993®

In the $[Fe(mtz)_6](BF_4)_2$ spin-crossover system, the Fe(II) complexes occupy two nonequivalent lattice sites. Complexes on lattice site A show a thermal high-spin (HS) → low-spin (LS) transition at 74 K, whereas complexes on site B remain in the high-spin state down to 10 K. Complexes on both sites exhibit light-induced spin-state conversions at 20 K: LS → HS on site A after irradiation at 514.5 nm; HS → LS on site B after irradiation at 830 nm. The subsequent relaxation processes are strongly influenced by cooperative effects of elastic origin, leading to characteristic deviations from first-order kinetics. This is attributed to a buildup of an internal pressure during the relaxation process, giving rise to a shift in both the horizontal (bond length difference Δr_{HL}) and the vertical (energy gap ΔE^0_{HL}) displacements of the potential wells of the two states relative to each other. The shifts can be estimated from the observed shift of the d–d absorption bands on the order of 100 cm^{-1}. For site B complexes, this may lead to a change in the true ground state.

Introduction

The series of compounds $[Fe(Rtz)_6](BF_4)_2$ (Rtz = 1-alkyltetrazole) are so-called spin-crossover compounds,[1,2] exhibiting an entropy-driven spin transition from the true low-spin (LS) $^1A_1$ ground state at low temperatures to the high-spin (HS) $^5T_2$ state at elevated temperatures. The detailed spin-crossover behavior varies with the substituent R and is strongly influenced by cooperative effects[3,4] of elastic origin due to the large difference in metal–ligand bond length $\Delta r_{HL} = r_{HS} - r_{LS}$ of 0.16–0.21 Å[5–7] or rather the concomitant difference in volume $\Delta V_{HL} = V_{HS} - V_{LS}$ of up to 50 Å^3 per complex[8] between the two states. The propyl derivative $[Fe(ptz)_6](BF_4)_2$, for instance, shows a quantitative spin transition, which is accompanied by a first-order crystallographic phase transition.[1,2] In the methyl derivative $[Fe(mtz)_6](BF_4)_2$, space group $P2_1/n$, the Fe(II) complexes occupy two nonequivalent lattice sites.[9] Only complexes on the one site, henceforth referred to as site A, show a steep thermal spin transition at 74 K, whereas complexes on the other site, site B, remain in the HS state down to 10 K,[10] indicating that the true ground state of the latter is the HS state.

The phenomenon of a light-induced LS → HS conversion at temperatures well below the thermal transition temperature was discovered for $[Fe(ptz)_6](BF_4)_2$.[11] The complete scheme for the large number of intersystem crossing (isc) processes, shown in Figure 1, was in fact fully established using the $[Fe(ptz)_6](BF_4)_2$ system.[12] The metastable HS state can be formed quantitatively by irradiating either into the spin-allowed $^1A_1 \rightarrow {}^1T_1$ or the spin-forbidden $^1A_1 \rightarrow {}^3T_1$ absorption bands of the LS species. The system can be pumped back to the LS state by irradiating into the spin-allowed $^5T_2 \rightarrow {}^5E$ absorption band of the HS species. The same holds for A site complexes in the $[Fe(mtz)_6](BF_4)_2$ system. In addition, Poganiuch et al.[10] achieved a partial light-induced HS → LS conversion and thus created a metastable LS state for complexes on site B. In their Mössbauer study, broad-band irradiation with $\lambda > 700$ nm gave a LS population on site B of 62%, as well as reducing the LS population on site A from the initial 100% to 62%. These populations are to be regarded as steady-state populations, resulting from the overlapping absorption bands of the LS and the HS species and the isc processes involved.

At low temperatures, the light-induced metastable states are very long-lived. In the $[Fe(ptz)_6](BF_4)_2$ system, for instance, the lifetime of the HS state at 20 K is $>10^6$ s. The HS → LS relaxation at $T > 50$ K deviates strongly from first-order kinetics.[11,13] Qualitatively, the elastic interactions lead to a buildup of an internal pressure during the relaxation process, resulting in self-accelerating, sigmoidal relaxation curves. A shift in the maxima of the d–d absorption bands of around 200 cm^{-1} indicates that there is a substantial increase in the zero-point energy difference $\Delta E^0_{HL} = E^0_{HS} - E^0_{LS}$ during the relaxation process. The HS → relaxation rates depend crucially upon the relative horizontal and vertical displacement of the two potential wells relative to each other. The sigmoidal relaxation curves could be explained quantitatively[14] on the basis of the inverse energy gap law from the theory of nonadiabatic multiphonon relaxation in the strong vibronic coupling limit.[15]

In this paper we report the HS → LS relaxation curves for

---

* Abstract published in *Advance ACS Abstracts*, January 1, 1994.

(1) Franke, P. L.; Haasnoot, J. G.; Zuur, A. P. *Inorg. Chim. Acta* **1982**, *59*, 5.
(2) Müller, E. W.; Ensling, J.; Spiering, H.; Gütlich, P. *Inorg. Chem.* **1983**, *22*, 2074.
(3) Slichter, C. P.; Drickamer, H. G. *J. Chem. Phys.* **1972**, *56*, 2142.
(4) Spiering, H.; Meissner, E.; Köppen, H.; Müller, E. W.; Gütlich, P. *Chem. Phys.* **1982**, *68*, 65.
(5) Hoselton, M. A.; Wilson, L. J.; Drago, R. S. *J. Am. Chem. Soc.* **1975**, *97*, 1722.
(6) Katz, B. A.; Strouse, C. E. *J. Am. Chem. Soc.* **1979**, *101*, 3744.
(7) Mikami-Kido, M.; Saito, Y. *Acta Crystallogr.* **1982**, *B38*, 452.
(8) Wiehl, L.; Spiering, H.; Gütlich, P.; Knorr, K. *J. Appl. Crystallogr.* **1990**, *23*, 151.
(9) Wiehl, L. *Acta Crystallogr.* **1993**, *B49*, 289.
(10) Poganiuch, P.; Decurtins, S.; Gütlich, P. *J. Am. Chem. Soc.* **1990**, *112*, 3270.
(11) Decurtins, S.; Gütlich, P.; Hasselbach, K. M.; Spiering, H.; Hauser, A. *Inorg. Chem.* **1985**, *24*, 2174.
(12) Hauser, A. *J. Chem. Phys.* **1991**, *94*, 2741.
(13) Hauser, A.; Gütlich, P.; Spiering, H. *Inorg. Chem.* **1986**, *25*, 4345.
(14) Hauser, A. *Chem. Phys. Lett.* **1992**, *192*, 65.
(15) Buhks, E.; Navon, G.; Bixon, M.; Jortner, J. *J. Am. Chem. Soc.* **1980**, *102*, 2918.

0020-1669/94/1333-0567$04.50/0

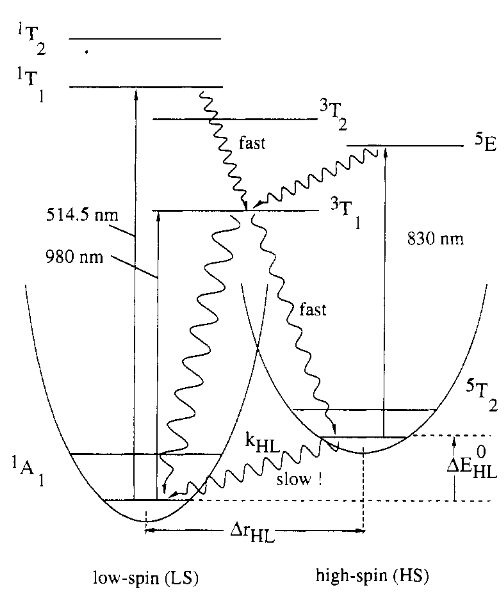

Figure 1. Potential wells of the $^1A_1$ ground state and the thermally accessible $^5T_2$ state as well as the higher excited ligand field states for a d^6 spin-crossover system. Arrows indicate the mechanism for the light-induced spin-state conversion.

complexes on site A and LS → HS relaxation curves for complexes on site B in the $[Fe(mtz)_6](BF_4)_2$ spin-crossover system. In particular, it is shown that a change in the true ground state of the B site complexes can be induced by the internal pressure resulting from the elastic interactions.

Experimental Section

Sample Preparation. The 1-methyltetrazole (mtz) ligand was prepared as described in ref 1. $[Fe(mtz)_6](BF_4)_2$ itself was prepared according to refs 1 and 10. Single crystals in the form of colorless hexagonal plates of up to several millimeters in diameter and up to 1 mm thick were grown from nitromethane by slow evaporation in a stream of oxygen-free dry nitrogen at 293 K.

Optical Spectroscopy. Single-crystal absorption spectra were recorded with a UV/vis near-IR spectrometer (Bruins Instruments, Omega-10). Sample temperatures down to 10 K were achieved with a cold helium gas flow technique.

Irradiation experiments were performed with an Ar laser (Spectra-Physics 2020) at 514.5 nm and with a Ti–sapphire laser (Spectra-Physics 3900) at 830 nm. Laser powers used were of the order of a few tens of a milliwatt with irradiation times of a few minutes.

In the temperature range under consideration, relaxation processes are slow. The crystals were kept at the temperature at which the relaxation curve was to be recorded throughout the irradiation, and the relaxation was monitored by recording full absorption spectra at appropriate time intervals after switching off the laser.

Results

Light-Induced Spin Transitions in $[Fe(mtz)_6](BF_4)_2$. At 20 K, the optical absorption spectrum of $[Fe(mtz)_6](BF_4)_2$ (Figure 2a) consists of the typical $^1A_1 \rightarrow {}^1T_1$ and $^1A_1 \rightarrow {}^1T_2$ absorption bands in the visible region, corresponding to site A complexes, and the $^5T_2 \rightarrow {}^5E$ band in the near-IR region of the site B complexes. Irradiation at 514.5 nm, that is into the $^1A_1 \rightarrow {}^1T_1$ absorption band, results in a quantitative light-induced LS → HS conversion on site A. This follows from the optical absorption spectrum in Figure 2b, in which the characteristic bands of the LS species have disappeared completely and the HS band has grown in intensity.

As can be seen from the optical absorption spectrum in Figure 2c, irradiation at 830 nm and 20 K results in an overall increase of the LS fraction γ_{LS} to approximately 82%. This is mainly due to a light-induced HS → LS conversion on site B. But, as in the propyl derivative,[12] this process is not quite quantitative. Because of the overlapping bands of the spin-allowed $^5T_2 \rightarrow {}^5E$ transition of the HS species and the spin-forbidden $^1A_1 \rightarrow {}^3T_1$ and $^1A_1 \rightarrow {}^3T_2$ transitions of the LS species, the corresponding isc processes lead to a steady-state LS fraction of less than unity. For irradiation at 830 nm, that is at the maximum of the $^5T_2 \rightarrow {}^5E$ band, a maximum steady-state LS fraction is obtained. Of course, the same thing applies to site A as well, with the difference that starting with the complexes in the LS state requires a small fraction to be converted to the HS state in order to reach the steady state. That this is indeed the case is borne out by the Mössbauer spectra of Poganiuch et al.,[10] showing approximately equal LS fractions on both sites, except that, for broad-band irradiation with $\lambda >$ 700 nm, the overall steady LS fraction of 62% is somewhat lower than that for the laser irradiation.

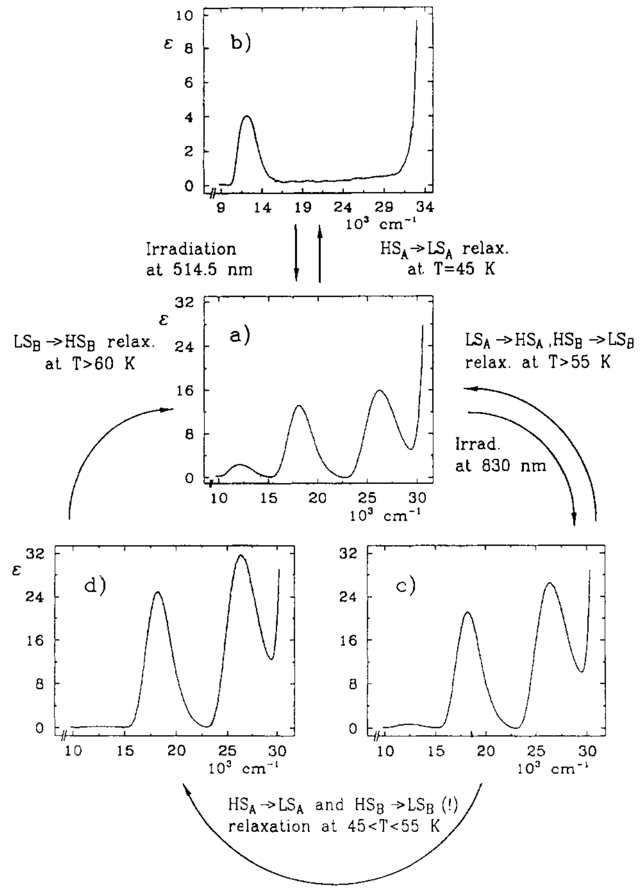

Figure 2. Single-crystal absorption spectra of $[Fe(mtz)_6](BF_4)_2$ at 20 K: (a) before irradiation ($\gamma_{LS} = 0.5$); (b) after irradiation at 514.5 nm ($\gamma_{LS} = 0$); (c) after irradiation at 830 K ($\gamma_{LS} = 0.82$); (d) after warming to 55 K in stages as described in the text ($\gamma_{LS} = 0.95$).

Relaxation Processes. (a) HS → LS Relaxation at Site A. At 20 K, the lifetime of the light-induced metastable HS state created on site A by irradiating at 514.5 nm is $>10^6$ s. At $T \geq 45$ K, a HS → LS relaxation process sets in. Figure 3a shows the $^1A_1 \rightarrow {}^1T_1$ band growing in intensity with time at 64 K after the laser has been switched off. Plotting the relative intensity against time results in the HS → LS relaxation curve for site A complexes displayed in Figure 4a. It should be remembered that, during the HS → LS relaxation on site A, all the complexes on site B are in the HS state, that is $\gamma_{LS}^B = 0$, while the LS fraction on site A goes from $\gamma_{LS}^A(t = 0) = 0$ to $\gamma_{LS}^A(t \rightarrow \infty) = 1$. Therefore the total LS fraction $\gamma_{LS} = {}^1/_2(\gamma_{LS}^A + \gamma_{LS}^B)$ goes from 0 to 0.5. As in the propyl derivative, the HS → LS relaxation is self-accelerating and can be described phenomenologically with a rate constant k_{HL}^A depending upon the LS fraction according to[14]

$$k_{HL}^A(\gamma_{LS}^A) = k_{HL}^{o} \exp(a\gamma_{LS}^A) \qquad (1)$$

A numerical fit to the experimental curve results in values for a of 2.25(3) and k_{HL}^{o} of $1.63(4) \times 10^{-4}$ s^{-1}.

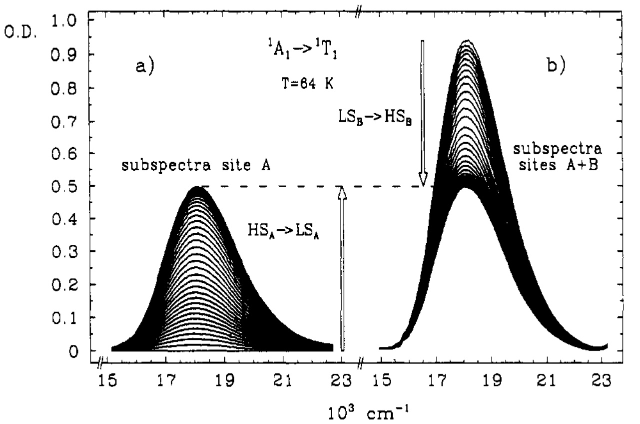

Figure 3. Single-crystal absorption spectra of [Fe(mtz)$_6$](BF$_4$)$_2$ showing (a) the recovery of the $^1A_1 \rightarrow {}^1T_1$ absorption band at 64 K after irradiation at 514.5 nm (time interval 240 s) and (b) the decreasing intensity of the $^1A_1 \rightarrow {}^1T_1$ absorption band after irradiation at 830 nm and warming the sample to 64 K in stages (time interval 360 s).

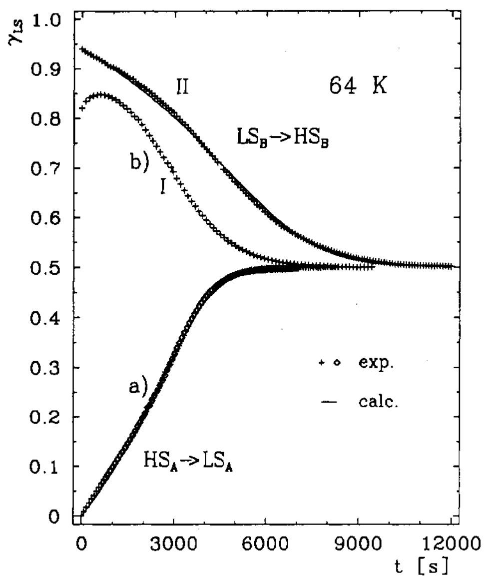

Figure 4. Relaxation curves γ_{LS} versus t at 64 K: (a) HS$_A$ → LS$_A$ relaxation after irradiation at 514.5 nm (+) and after rapidly cooling down (O); (b) LS$_B$ → HS$_B$ relaxation after irradiation at 830 nm, after warming up directly (type I) and after warming up in stages (type II).

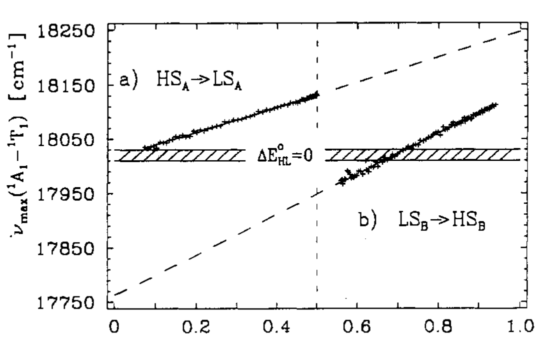

Figure 5. Shift of the $^1A_1 \rightarrow {}^1T_1$ absorption band as a function of the LS fraction γ_{LS} during (a) the HS$_A$ → LS$_A$ relaxation and (b) the LS$_B$ → HS$_B$ relaxation at 64 K: (+) experimental points; (- - -) linear regression; (a) $\nu^A_{max}(\gamma_{LS} = 0.5)$ = 18 130(10) cm^{-1}, slope $\Delta\nu^A_{max}$ = 23 0(5) cm^{-1}; (b) $\nu^B_{max}(\gamma_{LS} = 0.5)$ = 17 950(12) cm^{-1}, slope $\Delta\nu^B_{max}$ = 372(8) cm^{-1}.

Careful analysis of the position of the band maximum of the $^1A_1 \rightarrow {}^1T_1$ transition reveals a small but significant shift during the relaxation process. This shift, shown in Figure 5 as a function of the total γ_{LS}, is found to be linear in γ_{LS} with a slope $\Delta\nu^A_{max}$ = 230(5) cm^{-1} and a value of ν^A_{max} = 18 130(10) cm^{-1} for the maximum at the end of the relaxation.

Because the HS → LS relaxation at the thermal-spin-transition temperature of 74 K is quite slow, the sample can be frozen in the HS state not only by irradiation but also by rapid cooling. Included in Figure 4 is the relaxation curve at 64 K for the temperature-quenched HS state. It is within experimental error identical to the relaxation curve obtained after the light-induced population of the metastable HS state. In this system, with no added complications arising from crystallographic phase transitions, the manner in which the metastable HS state is prepared does not influence the HS → LS relaxation.

(b) LS → HS Relaxation at Site B. The relaxation processes after irradiation at 830 nm are somewhat more complicated. Warming the sample from 20 K to $T > 60$ K directly results in a relaxation curve of type I, as shown in Figure 4 for a temperature of 64 K. Obviously, the small HS fraction on site A created by the irradiation at 830 nm (via $^1A_1 \rightarrow {}^3T_{1,2} \rightarrow {}^5T_2$) decays more rapidly than the metastable LS fraction on site B, thus causing the initial increase in the total LS fraction. Unfortunately, at 64 K the relaxation processes are too fast to be monitored by Mössbauer spectroscopy, and with optical methods it is not possible to properly disentangle them at this stage.

If the sample is warmed up to $T > 60$ K in stages, something quite surprising happens, depending upon the initial LS population. In the Mössbauer study of Poganiuch et al.[10] with an initial LS population of 62%, obtained after broad-band irradiation with $\lambda > 700$ nm, a very slow HS$_A$ → LS$_A$ relaxation was observed to set in at $T \approx 45$ K, followed by the LS$_B$ → HS$_B$ relaxation at $T \approx 55$ K. In our experiment with an initial LS population of 82% after narrow-band irradiation at 830 nm, the HS$_A$ → LS$_A$ relaxation is as before, but if in the second stage the sample is warmed to $T \approx 55$ K, it is not the expected LS$_B$ → HS$_B$ relaxation which sets in; much rather, the remaining HS complexes on site B go to the LS state as well! In the corresponding optical spectrum of Figure 2d, the $^5T_2 \rightarrow {}^5E$ absorption band has disappeared completely, whereas the intensity of the $^1A_1 \rightarrow {}^1T_1$ band has become twice as large as in Figure 2a. Warming the sample to $T > 60$ K in a third stage now results in a relaxation curve of type II, as shown in Figure 4 for $T = 64$ K. This curve, obtained from the optical spectra of Figure 3b, corresponds to a clean LS → HS relaxation on site B. Similar to the HS → LS relaxation on site A, it is self-accelerating with a rate constant given by

$$k^B_{LH}(\gamma^B_{HS}) = k^o_{LH}\exp(b\gamma^B_{HS}) \qquad (2)$$

A numerical fit yields b = 2.69(3), which is somewhat larger than a = 2.25(3) for the HS → LS relaxation on site A, and $k^o_{LH} = 6.34(4) \times 10^{-5}$ s^{-1}. The optical spectra of Figure 3b, too, show a small shift of the band maximum during the relaxation. Of primary interest is not this shift itself but the shift of the subspectrum from complexes on site B. It would of course be wrong to just subtract the spectrum for $t \rightarrow \infty$ from Figure 3a as subspectrum for complexes on site A, because the increasing internal pressure due to the nonzero LS fraction on site B also acts on complexes on site A, shifting their subspectrum toward higher energy, but without changing its intensity. Since the two sites are geometrically very similar,[9] it is fair to assume that the internal pressure depends basically upon the total LS fraction and that therefore subspectrum A continues to be shifted linearly toward higher energy even for $\gamma_{LS} > 0.5$. As illustrated schematically in Figure 6, subspectrum B can thus be obtained by subtracting subspectrum A for $t \rightarrow \infty$ from Figure 3a, shifted according to the total LS fraction, from the experimental spectrum. The resulting band maximum as a function of γ_{LS} during the LS$_B$ → HS$_B$ relaxation is displayed in Figure 5. It, too, is linear in γ_{LS} with a slope of $\Delta\nu^B_{max}$ = 372(8) cm^{-1} and a value of ν^B_{max} = 17 950(12) cm^{-1} at $t \rightarrow \infty$, which is just 180 cm^{-1} less than ν^A_{max}.

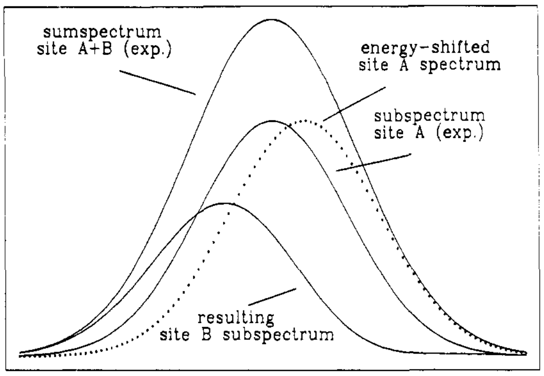

Figure 6. Schematic illustration of the procedure adopted to determine the shift of the $^1A_1 \rightarrow {}^1T_1$ absorption band of site B complexes during the $LS_B \rightarrow HS_B$ relaxation.

Discussion

The steep thermal spin transition at 74 K for complexes on site A indicates that cooperative effects of elastic origin[4,16,17] are important in the $[Fe(mtz)_6](BF_4)_2$ spin-crossover system. The purpose of this paper, however, is not to discuss these effects on the thermal spin transition but to show that they are responsible for the unusual relaxation behavior observed in $[Fe(mtz)_6](BF_4)_2$.

The cooperative effects are attributed to a buildup of an internal pressure acting on each individual complex as a result of the large difference in metal–ligand bond length Δr_{HL} or rather the large difference in volume ΔV_{HL} between complexes in the HS and in the LS state. In the most simple, isotropic model,[4] this internal pressure increases linearly with the total LS fraction, and as a consequence, the horizontal as well as the vertical displacements of the potential wells of the two states relative to each other depend upon the LS fraction in much the same way as they do upon application of an external pressure.[18]

Fine-Tuning the Energy Gap by Internal Pressure. With a thermal transition temperature $T_{1/2} = 74$ K, the zero-point energy difference ΔE^0_{HL} for site A complexes is small but certainly larger than zero at all times. For the 20 K thermodynamically stable phase, that is with $\gamma_{LS} = 0.5$ ($\gamma^A_{LS} = 1$, $\gamma^B_{LS} = 0$), ΔE^0_{HL} for B site complexes is less than zero, since they show no thermal spin transition. But it cannot be much smaller than zero, because the two sites are geometrically very similar. What then is the difference in ΔE^0_{HL} between the two sites? Well, in a first step the ligand field (LF) strength $10Dq$ or rather the difference in LF strengths between the two states can be derived from the experimental data. Because of the r^{-6} dependence, the LF strength differs by a factor of ~1.7 between the HS and the LS state.[12] Therefore, in order to be meaningful, the LF strengths for the two sites in the same spin state, e.g. the LS state, have to be compared. Furthermore, since the absorption bands shift with the total LS fraction γ_{LS}, this has to be done at some specific conditions, for instance at 20 K in the thermodynamically stable phase. The LF strength for site A complexes in the LS state $10Dq^A_{LS}$ has been estimated from the spin-allowed d–d transition energies by Poganiuch et al.[10] to be ≈20 200 cm^{-1}. Of course, the corresponding transition energies for B site complexes in the LS state at $\gamma^B_{LS} = 0$ cannot be measured directly. However, the difference in LF strength between the two sites $\Delta 10Dq_{LS} = 10Dq^A_{LS} - 10Dq^B_{LS}$ can be estimated from Figure 5 to be approximately equal to $\nu^A_{max} - \nu^B_{max} \approx 180$ cm^{-1}. The INDO–SCF–MO calculations of Clack and Smith[19] showed that there is a linear relationship with slope 1 between $10Dq_{LS}$ and ΔE^0_{HL}, and therefore ΔE^0_{HL} for B site complexes is ~180 cm^{-1} smaller than it is for A site complexes.

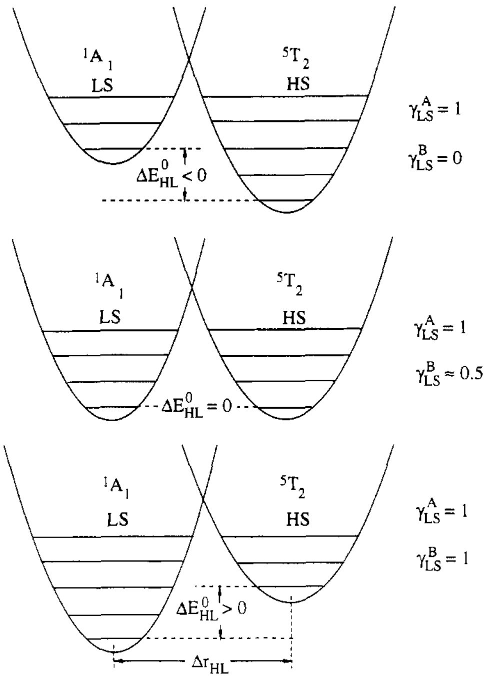

Figure 7. Fine-tuning of the energy gap ΔE^0_{HL} on site B complexes by internal pressure.

As mentioned above, ΔE^0_{HL} at $\gamma_{LS} = 0.5$ is >0 for A site complexes and <0 for B site complexes. The LF strength resulting in $\Delta E^0_{HL} \approx 0$ must therefore correspond to a transition energy of the $^1A_1 \rightarrow {}^1T_1$ transition between ν^A_{max} and ν^B_{max}, as indicated in Figure 5. The shift of the band maxima of the $^1A_1 \rightarrow {}^1T_1$ transition toward higher energy with increasing γ_{LS} indicates that $10Dq_{LS}$ and thus ΔE^0_{HL} increase with γ_{LS}, in accordance with the increasing pressure favoring the LS state. For A site complexes nothing spectacular happens, the increasing ΔE^0_{HL} just being the reason for the steep thermal transition curve and the sigmoidal $HS_A \rightarrow LS_A$ relaxation curves to be discussed in detail later. The light-induced population of the initially metastable LS state for B site complexes, on the other hand, has some interesting consequences: At a total LS fraction γ_{LS} below a critical value $\gamma^{crit}_{LS} \approx 0.75$, ΔE^0_{HL} for B site complexes is still <0, and upon warming to 55 K, just the straightforward $LS_B \rightarrow HS_B$ relaxation sets in, as observed upon broad-band irradiation with $\lambda > 700$ nm.[10] But for γ_{LS} above this critical value ΔE^0_{HL} becomes >0; that is, the LS state is now the true ground state for site B complexes too, as illustrated in Figure 7. Thus the fine-tuning of ΔE^0_{HL} by the elastic interactions is responsible for the observed $HS_B \rightarrow LS_B$ relaxation at 55 K after narrow-band irradiation at 830 nm.

The Sigmoidal Relaxation Curves. In the $[Fe(ptz)_6](BF_4)_2$ spin-crossover system, the HS → LS relaxation was first discussed using an empirical model with an activation energy E^a depending linearly upon the LS fraction as a consequence of the buildup of an internal pressure during the relaxation.[13] However, at that stage, it was not clear how an internal pressure, estimated to be of the order of kilobars, could lower the effective energy barrier between the potential wells of the two states to any large extent, because the change in Δr_{HL} due to such a pressure would only be of the order of ≈10^{-3} Å. As was later shown for $[Fe(ptz)_6](BF_4)_2$[14] and is explained in detail in the preceding section, it is not so much Δr_{HL} which is subject to large changes but rather

---

(16) Adler, P.; Wiehl, L.; Meissner, E.; Köhler, C. P.; Spiering, H.; Gütlich, P. *J. Phys. Chem. Soc.* **1987**, *48*, 517.

(17) Jakobi, R.; Spiering, H.; Wiehl, L.; Gmelin, E.; Gütlich, P. *Inorg. Chem.* **1988**, *27*, 1823.

(18) Drickamer, H. G.; Frank, C. W. *Electronic transitions and the high pressure chemistry and physics of solids*; Chapman and Hall: London, 1973.

(19) Clack, D. W.; Smith, W. E. *J. Chem. Soc.* **1974**, 2015.

the energy gap ΔE^0_{HL} which is a function of the LS fraction γ_{LS}. Since the HS → LS relaxation is a nonadiabatic process, classical concepts are not really adequate for its description anymore, especially at low temperatures, where tunneling processes become important.[20,21]

In the theory of nonadiabatic multiphonon relaxation,[15] the rate constant for an intersystem crossing process is given by[22]

$$k_{isc} = \frac{2\pi}{\hbar^2\omega}\beta_{isc}{}^2 g_f F_p(T) \qquad (3)$$

with the electronic matrix element $\beta_{isc} = \langle\Phi_{LS}|H_{SO}|\Phi_{HS}\rangle \approx 150$ cm^{-1} [15] for the $\Delta S = 2$ isc process in Fe(II) systems. The electronic degeneracy of the final state g_f is equal to 1 for the HS → LS relaxation and equal to 15 for the LS → HS relaxation. For harmonic potentials with equal force constants f and equal vibrational frequencies ω, the thermally averaged Franck–Condon factor $F_p(T)$ takes the form[22]

$$F_p(T) = \frac{\sum_m |\langle\chi_n|\chi_m\rangle|^2 \exp(-m\hbar\omega/k_B T)}{\sum_m \exp(-m\hbar\omega/k_B T)} \qquad (4)$$

The reduced energy gap $p = \Delta E^0_{if}/\hbar\omega$ is a measure for the vertical displacement of the potential wells of the initial and final states relative to each other. The sum goes over all the vibrational levels m of the initial state, and the vibrational level of the final state $n = m + p$, in order to ensure energy conversation. For $T \rightarrow 0$, F_p simplifies to

$$F_p(T) = |\langle\chi_p|\chi_0\rangle|^2 = \frac{S^p e^{-S}}{p!} \qquad (5)$$

where the Huang–Rhys factor $S = {}^1/_2 f(\Delta Q_{HL})^2/\hbar\omega$ is a measure for the relative horizontal displacement of the potential wells. For Fe(II) coordination compounds, a value for S of ≈ 45 has been estimated,[21] and with an average vibrational frequency of ≈ 250 cm^{-1} [2] for the metal–ligand stretch, $|p| < 1$ for the $[Fe(mtz)_6](BF_4)_2$ system. In the so-called strong-coupling limit with $S \gg p$, the characteristic features of $k_{isc}(T)$ are a temperature-independent tunneling rate below ≈ 50 K and a thermally activated process at elevated temperatures. In particular, the low-temperature tunneling rate $k_{isc}(T \rightarrow 0)$ is predicted to increase exponentially with increasing p:

$$k_{isc}(T \rightarrow 0) \approx k^0_{isc} \exp(\alpha p) \qquad (6)$$

with $\alpha \approx 4$–5 $(\geq \ln(S))$.[14] The analytical form of eq 6 is still approximately valid at elevated temperatures, but with the value for α dropping as $1/T$ above ≈ 50 K.

Thus if the energy gaps $\Delta E^0_{HL(A)}$ and $\Delta E^0_{HL(B)}$ of the two sites are functions of the LS fraction, the relaxation rates for the $HS_A \rightarrow LS_A$ and the $LS_B \rightarrow HS_B$ relaxation will obviously depend upon the LS fraction as well. Now, according to Figure 5, ΔE^0_{HL} for both sites is a linear function of the total LS fraction γ_{LS}. With the individual LS and HS fractions γ^A_{LS} and γ^B_{HS}, rather than the total LS fraction, $E^0_{HL(A)}$ and $\Delta E^0_{HL(B)}$ can be expressed as follows:

$$\Delta E^0_{HL(A)} = \Delta E^0_{HL(A)}(\gamma^A_{LS}{=}0) + {}^1/_2\Delta\nu^A_{max}\gamma^A_{LS} \qquad (7a)$$

with $\gamma^B_{LS} = 0$ and $\Delta\nu^A_{max} = 230$ cm^{-1} for the $HS_A \rightarrow LS_A$ relaxation, and

$$\Delta E^0_{HL(B)} = \Delta E^0_{HL(B)}(\gamma^B_{HS}{=}0) - 1/_2\Delta\nu^B_{max}\gamma^B_{HS} \qquad (7b)$$

with $\gamma^A_{HS} = 0$ and $\Delta\nu^B_{max} = 372$ cm^{-1} for the $LS_B \rightarrow HS_B$ relaxation. In terms of reduced energy gaps, eqs 7a and 7b can be recast as

$$p_A = \Delta E^0_{HL(A)}/\hbar\omega = p^0_A + {}^1/_2(\Delta\nu^A_{max}/\hbar\omega)\gamma^A_{LS} \qquad (8a)$$

$$p_B = -\Delta E^0_{HL(B)}/\hbar\omega = p^0_B + {}^1/_2(\Delta\nu^B_{max}/\hbar\omega)\gamma^B_{HS} \qquad (8b)$$

Inserting eqs 8a and 8b into eq 6 gives

$$k^A_{HL}(\gamma^A_{LS}) = k^o_{HL(A)} \exp(a\gamma^A_{LS}) \qquad (9a)$$

$$k^B_{LH}(\gamma^B_{HS}) = k^o_{LH(B)} \exp(b\gamma^B_{HS}) \qquad (9b)$$

with

$$a = {}^1/_2(\Delta\nu^A_{max}/\hbar\omega)\alpha \qquad (10a)$$

$$b = {}^1/_2(\Delta\nu^B_{max}/\hbar\omega)\alpha \qquad (10b)$$

Thus the energy gap law of eq 6 together with the experimentally determined linear dependence of the energy gap on the LS fraction justifies the phenomenological approach to the rate constants of eqs 1 and 2. Using values for α of ≈ 5 and for ω of ≈ 250 cm^{-1}, values for a and b of ≈ 2.5 and ≈ 3.5, respectively, can be estimated. These values hold for the low-temperature limit. As expected, the experimentally determined values at 64 K of 2.25 and 2.69, respectively, are slightly smaller than this. As predicted from the somewhat larger shift of the $^1A_1 \rightarrow {}^1T_1$ band for site B complexes as compared to the one for site A complexes (see Figure 5), the acceleration of the $LS_B \rightarrow HS_B$ relaxation is more pronounced than for the $HS_A \rightarrow LS_A$ relaxation.

Conclusions

The $[Fe(mtz)_6](BF_4)_2$ spin-crossover system is unique insofar as it is possible to actually determine the zero-point energy difference of the two sites from spectroscopic data. In the 20 K normal phase, that is with $\gamma_{LS} = 0.5$ ($\gamma^A_{LS} = 1$ and $\gamma^B_{LS} = 0$), $\Delta E^0_{HL(A)} \approx 120$ cm^{-1} and $\Delta E^0_{HL(B)} \approx -60$ cm^{-1}. With irradiation in the red, the LS state of site B complexes can be populated, at first as a metastable state but above some critical LS fraction as a thermodynamically stable state, because of the increasing internal pressure favoring the LS state. This system is thus truly bistable with respect to the B site complexes.

Basically the HS ⇔ LS relaxation in $[Fe(mtz)_6](BF_4)_2$ can still be treated at a single-molecule level, despite the fact that the relaxation curves deviate substantially from first-order kinetics. The cooperative effects due the large difference in volume between complexes in the HS and the LS state are accounted for by a varying internal pressure acting on a single complex molecule. Both the $HS_A \rightarrow LS_A$ relaxation and the $LS_B \rightarrow HS_B$ relaxation are self-accelerating, corresponding to an increasing pressure during the relaxation process favoring the LS state for the former and to a decreasing internal pressure favoring the HS state for the latter.

The simple form of eqs 1 and 2 for the rate constants results because of the exponential dependence of the rate constants on the zero-point energy difference in the limit of strong vibronic coupling, known as the "inverse energy gap law", and the linear dependence of the energy gap upon the LS fraction. It is quite gratifying to note that, despite the rather crude estimates of the vibrational frequency and the value for α, the quantitative agreement between theory and experiment is very reasonable.

Of course the simple picture of an internal pressure, depending linearly upon the LS fraction and acting basically upon the totally symmetric normal coordinate, is only valid in systems with very close to octahedral coordination, as is indeed the case for $[Fe(mtz)_6](BF_4)_2$.[9] In systems with lower symmetry, where the elastic forces are anisotropic,[23,24] an internal pressure is no longer a

---

(20) Xie, C.-L.; Hendrickson, D. N. *J. Am. Chem. Soc.* **1987**, *109*, 6981.
(21) Hauser, A.; Vef, A.; Adler, P. *J. Chem. Phys.* **1991**, *95*, 8710.
(22) Donnelly, C. J.; Imbush, G. F. *NATO ASI Ser., Ser. B* **1991**, *245*, 175.

meaningful concept. In such systems, a more complicated dependence of the electronic energy gap on the LS fraction and additional electronic splittings would result in quite different deviations from first-order kinetics.

Our model treats the cooperative effects as due to long-range elastic interactions. In principle nearest-neighbor interactions have to be considered as well,[25] but those are small in systems with separated individual complexes such as ours. The plateau, in our case, is essentially due to the difference in ΔE^0_{HL} between the two nonequivalent lattice sites. In systems with direct links between nearest neighbors, for instance those with hydrogen bonds[26] or those containing dinuclear complexes,[27] nearest-neighbor interactions do indeed become important. As was shown by Boussekson et al.,[28] an "antiferromagnetic" type of interaction may lead to a plateau in the thermal-spin-transition curve even in the case of no nonequivalent lattice sites. It would, of course, be most interesting to study the relaxation kinetics in such systems.

Acknowledgment. We thank H. Spiering and R. Jakobi for helpful discussions. This work was financially supported by the Schweizerische National Fonds and the Deutsche Forschungsgemeinschaft.

---

(23) Willenbacher, N.; Spiering, H. *J. Phys. C: Solid State Phys.* **1988**, *21*, 1423.

(24) Spiering, H.; Willenbacher, N. *J. Phys.: Condens. Matter* **1989**, *1*, 10089.

(25) Sasaki, N.; Kambara, T. *Phys. Rev. B* **1989**, *40*, 2442.

(26) Köhler, C. P.; Jakobi, R.; Meissner, E.; Wiehl, L.; Spiering, H.; Gütlich, P. *J. Phys. Chem. Solids* **1990**, *51*, 239.

(27) Real, J.-C.; Bolvin, H.; Bousseksou, A.; Dworkin, A.; Kahn, O.; Varret, F.; Zarembowitch, J. *J. Am. Chem. Soc.* **1992**, *114*, 4650.

(28) Bousseksou, A.; Nasser, J.; Linares, J.; Boukheddaden, K.; Varret, F. *J. Phys. I* **1992**, *2*, 1381.